NUMERICAL STUDY ON DYNAMIC WETTABILITY OF MICRO-STRUCTURE SURFACE

by

Shuang HAN[a,b], Lixin YANG[a,b*], Runhua YANG[c], and Zihao TIAN[a,b]

[a]Institute of Thermal Engineering, School of Mechanical, Electronic and Control Engineering, Beijing Jiaotong University, Beijing, China
[b]Beijing Key Laboratory of Flow and Heat Transfer of Phase Changing in Micro and Small Scale, Beijing, China
[c]Beijing Huanengda Power Technology Company, Beijing, China

Original scientific paper
https://doi.org/10.2298/TSCI19S4241H

Wettability plays a vital role in many fields. In this paper, the shortcomings of current experimental measurement of dynamic wetting characteristics are described. The dynamic wettability of droplets on the simplified triangular wave micro-structure surface is studied by volume of fluid method. The results are compared with the dynamic wettability of droplets on the smooth surface and the rectangular wave micro-structure surface. The results show the similarities and differences of the motion characteristics of droplets on smooth surface and different micro-structure surface. Under the action of volume force, the droplets are first deformed and then moved. The droplets move as a whole on the smooth surface. But the droplets partially slip on the micro-structure surface, and the three-phase contact point on the left side does not move.

Key words: *micro-structural surface, dynamic wettability, volume of fluid, numerical simulation*

Introduction

Wetting is the process that one fluid replaces another on a solid surface. Usually the liquid replaces the air. There are many wetting phenomena in nature. For example, droplets are spherical on canna leaves and rice leaves [1, 2]. The peristome surface of nepenthes makes insects unable to stop and slide into cages [3]. Some insect feathers are superhydrophobic [4]. According to these natural phenomena, people obtain new material that is beneficial to humans such as food packaging materials [5] and superhydrophobic or superhydrophilic fabrics [6]. At the same time, wettability plays a key role in petroleum exploitation [7], boiling [8], condensation [9], coating [10, 11], material [12, 13], inkjet printing [14, 15].

The study of wetting characteristics mainly included static wettability and dynamic wettability. The current research on wetting characteristics mainly included in theoretical, numerical and experimental studies. Jiao *et al* [16] studied the influence of the dynamic wettability of catalyst layer and gas diffusion layer on the liquid transport in proton exchange membrane fuel cell. Luo *et al* [17] used artificial saliva to research the static and dynamic

[*] Correspondence author, e-mail: lxyang1@bjtu.edu.cn

wettability of commercial vinyl polysiloxane impression materials. The material was applied in stomatology. Chen *et al* [18] summarized the study of dynamic wetting characteristics of soft substrates. Liu *et al* [19] got a wetting model to describe the wetting of the straw surface. Yan *et al.* [20] studied the contact state of the droplet on the surface of the nanoscale trench structure by means of molecular dynamics methods, and discussed the influence of a series of parameters such as the width and depth of the trench on the wetting mode and the contact angle. Huang *et al.* [21] studied the wettability of hydrophobic surfaces by means of the lattice Boltzmann method. Some scholars had used molecular dynamics and Boltzmann numerical simulation methods to study the influence of typical micro-structures on the contact angle. At present, they only focused on such regular micro-structures as trenches. These two numerical methods are not based on the study of the continuum media flow, they will bring great difficulties in the simulation prediction of the dynamic contact angle, and the two simulation methods require high computational resources.

For the dynamic wettability, the concepts of advancing contact angle, θ_A, receding contact angle, θ_R, contact angle hysteresis, $\Delta\theta$, and rolling angle, θ, are proposed. The advancing contact angle refers to the contact angle formed when the solid-gas interface is replaced by the liquid-solid interface in the process of wetting. And the receding contact angle is the contact angle formed when the liquid-solid interface is replaced by the solid-gas interface in the process of wetting. The contact angle hysteresis is the difference between the advancing contact angle and the receding contact angle [22, 23]. The smaller the contact angle hysteresis, the easier it is for the droplet to roll on the solid surface. The rolling angle is used to determine the difficulty of droplet moving on solid surface. A drop is placed on the horizontal solid surface. The solid surface is slowly tilted. Under the gravity of the droplet, the tilt angle of the surface when the droplet just starts to move on the surface is the rolling angle.

The contact angle hysteresis can be measured experimentally. The most common measurement method is to measure the advancing and receding contact angles of the droplet by adding/reducing the volume of the liquid, shown in fig. 1(a). Another commom method is to measure the advancing and receding contact angles of the droplet by the tilting plate method, shown in fig. 1(b). However, the dynamic contact angle is a parameter that is difficult to measure. The measurement results are affected by many factors. So the measured results by different measurement methods may be quite different.

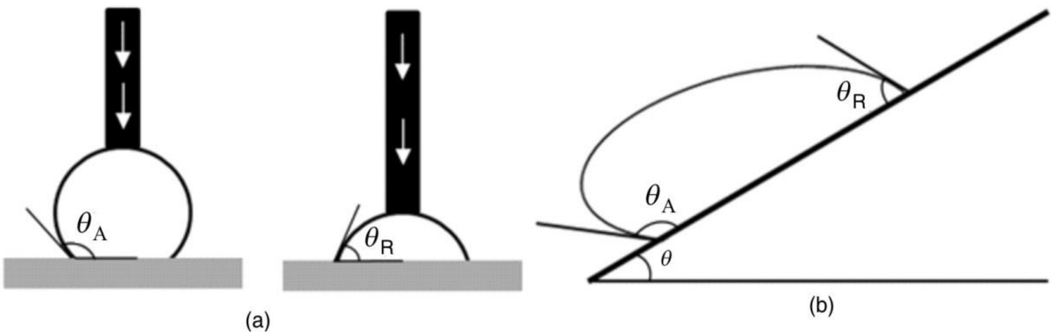

Figure 1. The measurement of the contact angle hysteresis; (a) adding/reducing the volume of the liquid method and (b) tilting plate method

In [24], it was concluded that the wettability of the droplet on triangular wave micro-structure surfaces calculated by volume of fluid (VOF) method was in good agreement with the wettability of the droplet on experimental silicon surfaces. Therefore, in this paper, the dynamic wettability of the triangular wave micro-structure surfaces was calculated by VOF method. The results were compared with the dynamic wettability of smooth surfaces and rectangular wave micro-structure surfaces. The similarities and differences of dynamic wettability of different parameterized micro-structure surfaces were obtained.

Analysis and modelling

Geometric model

The micro-structural surface was simplified and the parametric geometric model was established in [24] (as shown in fig. 2).

In this paper, the triangle wave of the [24] was selected as the geometric model of the typical micro-structure surface. The calculation model used a 2-D planar structure, as shown in fig. 2. The computational domain had a width of 300 μm and a height of 120 μm.

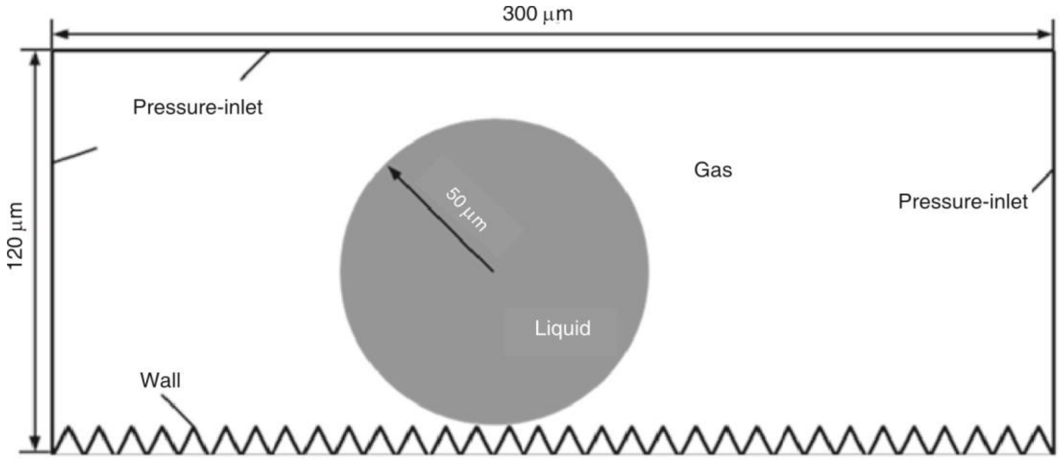

Figure 2. Geometric model and boundary condition

Mesh model

In this paper, ICEM CFD was used for mesh generation. The calculation area was divided into two areas including wall area and air area. The unstructured mesh was used. The mesh type was tetra/mixed meshing. At the same time, the prism mesh and the local mesh refinement was used in the wall area. The total elements of mesh was 270555. The total nodes of mesh was 263230. The mesh model was shown in fig. 3.

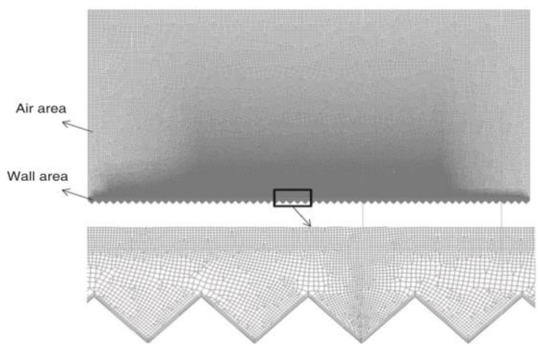

Figure 3. Mesh model

The VOF model

The VOF method is a surface tracking method based on fixed Euler mesh. It is based on the premise that two or more fluids (or phases) do not mix with each other. In

VOF model, different fluid components share a set of momentum equations. By introducing the variable of phase volume fraction, the phase interface of each calculation unit can be tracked. Within each control volume, the sum of all phase volume fractions is 1. In the paper, the value of the fluid volume fraction in one control volume was shown.

$\alpha = 0$ only air in the control unit

$0 < \alpha < 1$ water and air in the control unit

$\alpha = 1$ only water in the control unit

The momentum equations of the two phases were defined:

$$\frac{\partial}{\partial t}\left(\alpha_g \rho_g V_g\right) + \nabla\left(\alpha_g \rho_g \vec{v} V_g\right) = S + F \tag{1}$$

$$\frac{\partial}{\partial t}\left(\alpha_l \rho_l V_l\right) + \nabla\left(\alpha_l \rho_l \vec{v} V_l\right) = S + F \tag{2}$$

where script l was water and g was air, $\alpha_g + \alpha_l = 1$, S and F were the source term in the momentum equations, $S = \sigma/A$. The surface tension coefficient σ was determined to be 72.75 (mN/m), F was a horizontal to right volume force.

When the VOF method was used to simulate the dynamic wetting characteristics of micro-structural surfaces, the following assumptions were made:

– The fluid was a continuous medium in any area of the micro-structured surface.
– The Young's contact angle at any location on the micro-structure surface was the same as the macroscopic contact angle on the smooth surface.

Model verification

In [24], silicon surfaces of different micro-structures were fabricated by plasma immersion ion implantation technology. The micro-structure surfaces were simplified to obtain parametric micro-structure surfaces. The VOF method was used to calculate the wettability of the simplified triangular wave, rectangular wave and trapezoidal wave micro-structure surfaces. It was concluded that the calculation results of the triangular wave micro-structure surface were in good agreement with the experimental results. The comparison results were shown in fig. 4. Although the result of numerical simulation calculation was the static contact angles of droplets on different micro-structure surfaces, simulating the spreading process of droplets on different micro-structure surfaces by VOF method was a transient process. So it can be considered that the dynamic model of the droplet on the different micro-structure surfaces was sufficiently accurate.

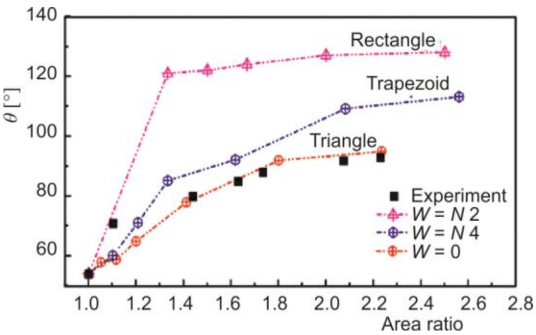

Figure 4. Experimental results and numerical simulation results of wettability [24]

Initial conditions and boundary conditions

The following assumptions in initial conditions were made:

– The initial water droplet shape was circle. The water droplet position was shown in fig. 2.

– The micro-structure channels were full of air, without water.

The initial the fluid volume fraction was:

$$\begin{cases} \alpha = 1 \ \left(r = 50 \ \mu\text{m}, 0 \le \theta \le 2\pi\right) \\ \alpha = 0 \ \left(\text{other region}\right) \end{cases} \tag{3}$$

The boundary conditions were shown in fig. 1. The surfaces of micro-structure had a contact angle of 54° [24], and the other boundaries were all set as the opening boundary with a pressure of 1 atm. The downward gravitational acceleration. The transient time step was 1×10^{-8} second.

Results and discussion

In order to simulate the motion of the droplets on the solid surface under the action of the body force, the body force of the horizontal to the right was given to droplets which reach the steady-state under the action of gravity. It promoted the movement of the droplet. In this paper, the motion of the droplets on the smooth surface and the micro-structure surface was calculated, respectively, to analyze the dynamic behavior of the droplets on the micro-structure surface.

The motion characteristics of droplets on triangular wave micro-structural surface

Figure 5 showed the motion of the droplets on the triangular surface under the action of the body force, the body force of the horizontal to the right was given to droplets which reached the steady-state. As shown in fig. 5(a), the steady-state of the droplet on the micro-structural surface under the action of gravity was a standard circular arc shape, and the contact angles at both ends of the droplet in contact with the micro-structural surface were equal. Under the horizontal rightward body force, the droplets begin to deform under the condition of keeping the liquid-solid contact line unchanged. The left contact angle become smaller and smaller, and the right contact angle become larger and larger as figs. 5(b) and 5(c) shown. When the contact angle on the right side of the droplet reached a certain value and did not change any more. It marked the end of the deformation stage of the droplet during its movement on the micro-structural surface. Then, under the body force and the surface tension, the droplets slided on the micro-structural surface when the right macroscopic contact angle remained basically unchanged, as shown in figs. 5(c)-5(f). However, the slippage of droplets on the micro-structure surface was not overall sliding, and the position of the gas-liquid-solid three-phase contact point on the left remained basically unchanged during the sliding of the droplets. This was because the micro-structural surface had a strong impediment to the movement of a layer of liquid on the left side wall. Therefore, with the sliding of some droplets, the advancing angle remained unchanged and the receding angle becomed smaller and smaller.

The motion characteristics of droplets on smooth surface

Figure 6 showed the motion of the droplets on the smooth surface under the action of the body force. Figure 6(a) showed the shape of droplets which reached the steady-state under gravity was standard circular arc, and the contact angles of the left and right ends contacting with the surface of the solid were equal. Then, under the influence of the body force, the droplets begined to deform. As shown in fig. 6(b), the shape of the droplet was no longer the standard circular arc shape, and the contact angles of the left and right ends contacting with the

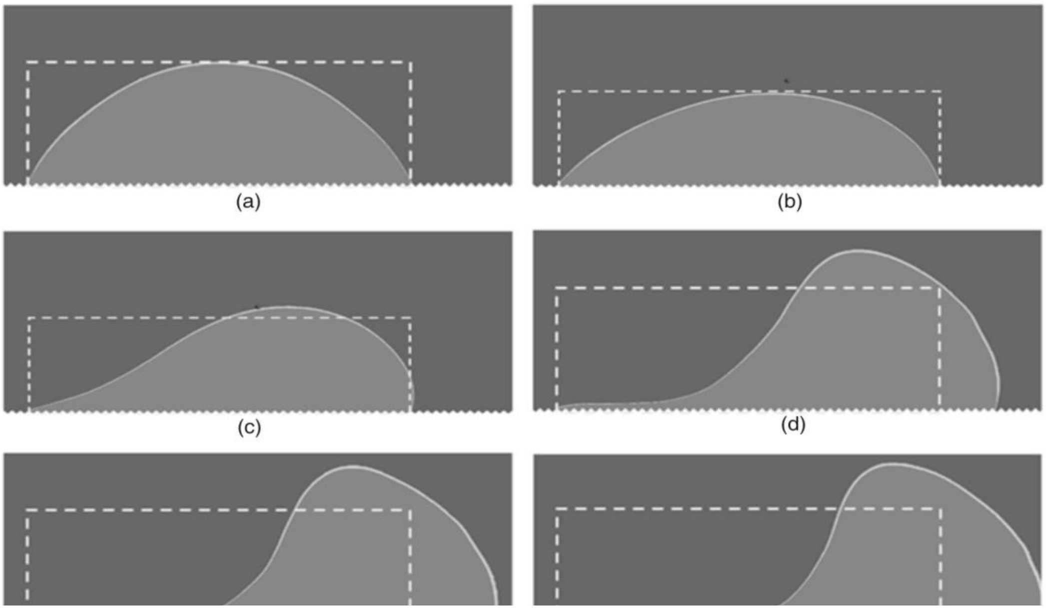

Figure 5. Motion behaviour of droplets on triangular wave micro-structural surface

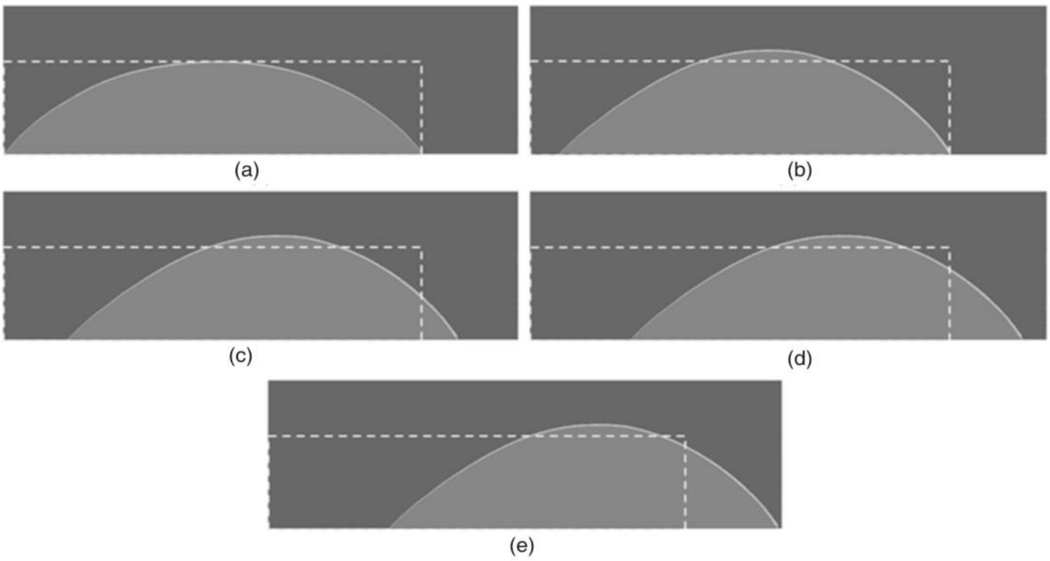

Figure 6. Motion behaviour of droplets on smooth surface

surface of the solid were no longer equal. The right contact point of the droplet contacting with the solid surface had not yet moved, but the left contact point moved to the right under the body force action, resulting in the right contact angle (advancing contact angle) greater than the left contact angle (retreat contact angle). The liquid contact line was shortened. Under the action of the body force, the droplet was continuously tilted to the right until the shape was as shown in fig. 6(b). The shape of the droplet no longer changed and started to slide to the right, as shown in figs. 6(b)-6(e). That was, the movement process of droplet on the smooth surface was composed of two stages: deformation and sliding. During the sliding process, the shape of the droplet did not change but the whole droplet moved forward uniformly. The macroscopic contact angles on the left and right sides of the droplet corresponded to the receding contact angle and advancing contact angle of the droplet on the smooth silicon surface, respectively.

The motion characteristics of droplets on rectangular wave micro-structural surface

Figure 7 showed the motion of the droplets on the rectangular wave micro-structural surface under the action of the body force. As shown in fig. 7(a), the steady-state of the droplet on the micro-structural surface under the action of gravity was a spherical cap shape, and the contact angles at both ends of the droplet in contact with the micro-structural surface were equal. The change process of the droplet on the rectangular wave micro-structure surface was consistent with the change process of the droplet on the triangular wave micro-structure surface.

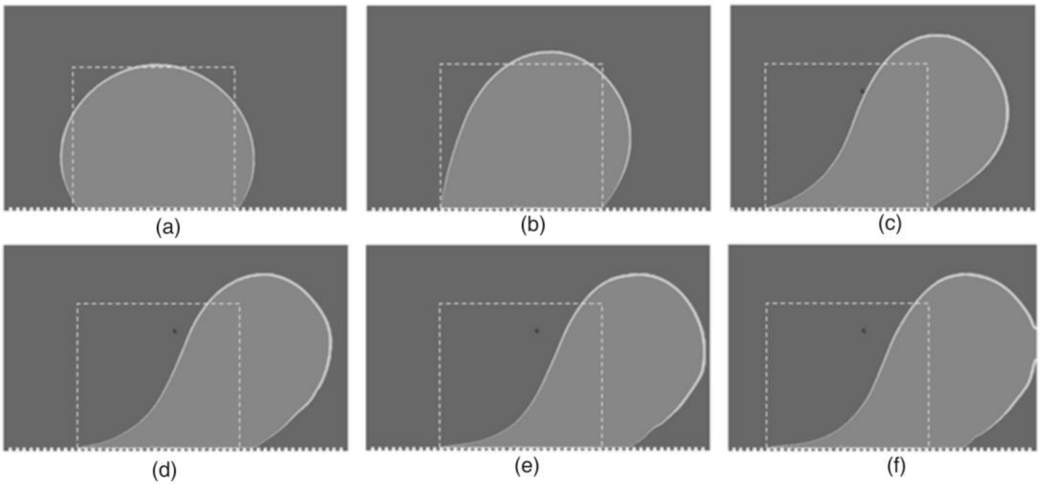

Figure 7. Motion behaviour of droplets on rectangular wave micro-structural surface

In summary, under the effect of the horizontal body force, the droplets firstly deform on a smooth surface and then form an overall uniform motion, and there are fixed forward and receding contact angles. The deformation of the droplet on the micro-structural surface can only make a part of the droplet slide. As the sliding progress, the receding angle approaches 0 continuously. The droplets on different micro-structural surface have different advancing contact angle characteristics.

Conclusions

According to the established numerical model of wettability, this paper analyses the motion characteristics of the droplet on the smooth surface and different micro-structure surface under the action of the body force. The main conclusions obtained are as follows.

- Under the action of body force, the droplet on the smooth surfaces and the micro-structure surfaces are first deformed and then slid.

- The droplet on the smooth surfaces slides as a whole, but the three-phase contact point on the left side of the droplet on the micro-structure surfaces do not move.
- The change process of the droplets on different micro-structure surfaces is similar. The receding contact angles of the droplets on different micro-structure surfaces tend to 0. However, different micro-structure surfaces have different advancing contact angle characteristics.

Nomenclature

F – volume force, [N]
S – source term, [Nm^{-3}]
t – time, [s]
V – velocity, [ms^{-1}]
$\vec{v}$ – speed vector, [ms^{-1}]

Greek symbols

α – phase volume fraction
θ – rolling angle, [°]
θ_A – advancing contact angle, [°]
θ_R – receding contact angle, [°]
$\Delta\theta$ – contact angle hysteresis, [°]
ρ – density, [kgm^{-3}]

Subscripts

g – air
l – water

References

[1] Guo, Z., *et al*., Biomimic from the Superhydrophobic Plant Leaves in Nature: Binary Structure and Unitary Structure, *Plant Science, 172* (2007), 6, pp. 1103-1112
[2] Guo, Z., *et al*., Progress in Biomimicing of Super-Hydrophobic Surface, *Progress in Chemistry, 18* (2006), 6, pp. 721-726
[3] Chen, H., *et al*., Continuous Directional Water Transport on the Peristome Surface of Nepenthes Alata, *Nature, 24* (2016), 3, pp. 85-89
[4] Ha, N. S., *et al*., Natural Insect and Plant Micro-/Nanostructsured Surfaces: an Excellent Selection of Valuable Templates with Superhydrophobic and Self-Cleaning Properties, *Molecules, 19* (2014), 9, pp. 13614-13630
[5] Zhang, Z., *et al*., Hydrophobic and Breathable Nanomembrane for Food Package Material by Mimicking Cocoon's Structure, *Thermal Science, 19* (2015), 4, pp. 1267-1271
[6] Liu, P., *et al*., Geometric Potential: An Explanation of Nanofiber's Wettability, *Thermal Science, 22* (2018), 1, pp. 33-38
[7] Alvarez, J. O., *et al*., Application of Wettability Alteration in the Exploitation of Unconventional Liquid Resource, *Petroleum Exploration & Development, 43* (2016), 5, pp. 832-840
[8] Betz., *et al*., Boiling Heat Transfer on Superhydrophilic, Superhydrophobic, and; Superbiphilic Surfaces, *International Journal of Heat & Mass Transfer, 57* (2013), 2, pp. 733-741
[9] Qi, B., *et al*., A Fractal Dropwise Condensation Heat Transfer Model including the Effects of Contact Angle and Drop Size Distribution, *International Journal of Heat & Mass Transfer, 83* (2015), Apr., pp. 259-272
[10] Pilotek, S., *et al*., Wettability of Micro-Structured Hydrophobic Sol-Gel Coatings, *Journal of Sol-Gel Science and Technology, 26* (2003), 1-3, pp. 789-792
[11] Oukach, S., *et al*., Numerical Study of the Spreading and Solidification of a Molten Particle Impacting onto a Rigid Substrate Under Plasma Spraying Conditions, *Thermal Science, 19* (2015), 1, pp. 277-284
[12] Hodgson, K. T., *et al*., Dynamic Wettability Properties of Single Wood Pulp Fibers and Their Relationship to Absorbency, *Wood & Fiber Science, 20* (1988), 1, pp. 3-17
[13] Wang, X., *et al*., Surface Free Energy and Dynamic Wettability of Wood Simultaneously Treated with Acidic Dye and Flame Retardant, *Journal of Wood Science, 63* (2017), 3, pp. 271-280
[14] Gennes, P. G. D., *et al*., Capillarity and Wetting Phenomena, *Physics Today, 57* (2004), 12, pp. 66-67
[15] Liu, M., *et al*., Inkjet Printing Controllable Footprint Lines by Regulating the Dynamic Wettability of Coalescing Ink Droplets, *Acs Applied Materials & Interfaces, 6* (2014), 16, pp. 13344-13348
[16] Jiao, K., *et al*., Effect of Surface Dynamic Wettability in Proton Exchange Membrane Fuel Cells, *International Journal of Hydrogen Energy, 35* (2010), 17, pp. 9095-9103
[17] Luo, F., *et al*., Static and Dynamic Evaluations of the Wettability of Commercial Vinyl Polysiloxane Impression Materials for Artificial Saliva, *Dental Materials Journal, 37* (2018), 5, pp. 818-824

[18] Chen, L., *et al*., Static and Dynamic Wetting of Soft Substrates, *Current Opinion in Colloid & Interface Science*, *36* (2018), July, pp. 46-57
[19] Liu, B., *et al*., Study on the Surface Dynamic Wettability of Rice Straw, In Proceedings of International Conference on Mechanical & Electronics Engineering, *Proceedings*, 2nd International Conference on Mechanical and Electronics Engineering, Kyoto, Japan, 2010, Vol. 2, pp. 353-356
[20] Yan, X., *et al*., Molecular Dynamics Simulations on Wettability of Nano-grooved Surface (in Chinese), *Atomic Energy Science and Technology, 49* (2015), 1, pp. 342-348
[21] Huang, Q. G., *et al*., Numerical Simulation on Wettability of Hydrophobic Surfaces Based on Lattice Boltzmann Method, *Journal of Functional Materials, 46* (2015), 10, pp. 10023-10028
[22] Nakajima, A., *et al*., Recent Studies on Super-Hydrophobic Films, *Monatshefte Für Chemie, 132* (2001), 1, pp. 31-41
[23] Rowell, R. L., Physical Chemistry of Surfaces, *Journal of Colloid & Interface Science, 208* (1998), 2, pp. 582-582
[24] Han, S., *et al*., The Wettability and Numerical Model of Different Silicon Micro-structural Surfaces, *Applied Sciences, 9* (2019), 566, pp. 1-16

Paper submitted: October 15, 2018
Paper revised: February 28, 2019
Paper accepted: March 21, 2019